Sorafenib Blocks the RAF/MEK/ERK Pathway, Inhibits Tumor Angiogenesis, and Induces Tumor Cell Apoptosis in Hepatocellular Carcinoma Model PLC/PRF/5

Li Liu, Yichen Cao, Charles Chen, Xiaomei Zhang, Angela McNabola, Dean Wilkie, Scott Wilhelm, Mark Lynch, and Christopher Carter

Department of Cancer Biology, Bayer HealthCare Pharmaceuticals, West Haven, Connecticut

Abstract

Angiogenesis and signaling through the RAF/mitogen-activated protein/extracellular signal-regulated kinase (ERK) kinase (MEK)/ERK cascade have been reported to play important roles in the development of hepatocellular carcinomas (HCC). Sorafenib (BAY 43-9006, Nexavar) is a multikinase inhibitor with activity against Raf kinase and several receptor tyrosine kinases, including vascular endothelial growth factor receptor 2 (VEGFR2), platelet-derived growth factor receptor (PDGFR), FLT3, Ret, and c-Kit. In this study, we investigated the *in vitro* effects of sorafenib on PLC/PRF/5 and HepG2 HCC cells and the *in vivo* antitumor efficacy and mechanism of action on PLC/PRF/5 human tumor xenografts in severe combined immunodeficient mice. Sorafenib inhibited the phosphorylation of MEK and ERK and down-regulated cyclin D1 levels in these two cell lines. Sorafenib also reduced the phosphorylation level of eIF4E and down-regulated the antiapoptotic protein Mcl-1 in a MEK/ERK–independent manner. Consistent with the effects on both MEK/ERK–dependent and MEK/ERK–independent signaling pathways, sorafenib inhibited proliferation and induced apoptosis in both HCC cell lines. In the PLC/PRF/5 xenograft model, sorafenib tosylate dosed at 10 mg/kg inhibited tumor growth by 49%. At 30 mg/kg, sorafenib tosylate produced complete tumor growth inhibition. A dose of 100 mg/kg produced partial tumor regressions in 50% of the mice. In mechanism of action studies, sorafenib inhibited the phosphorylation of both ERK and eIF4E, reduced the microvessel area (assessed by CD34 immunohistochemistry), and induced tumor cell apoptosis (assessed by terminal deoxynucleotidyl transferase–mediated nick end labeling) in PLC/PRF/5 tumor xenografts. These results suggest that the antitumor activity of sorafenib in HCC models may be attributed to inhibition of tumor angiogenesis (VEGFR and PDGFR) and direct effects on tumor cell proliferation/survival (Raf kinase signaling-dependent and signaling-independent mechanisms). (Cancer Res 2006; 66(24): 11851-8)

Introduction

Hepatocellular carcinoma (HCC) is the fifth most common cancer in the world and is responsible for >600,000 deaths annually (1). The majority of patients with HCC die within 1 year after the diagnosis of their disease. Unfortunately, the disease is often diagnosed at a late stage when potentially curative therapies are least effective. For these patients, medical treatments, including chemotherapy, chemoembolization, ablation, and proton beam therapy, remain disappointing. Most patients show disease recurrence that rapidly progresses to the advanced stages with vascular invasion and multiple intrahepatic metastases and their 5-year relative survival rate is only 7% (2). The prognosis for HCC patients who have surgically resectable localized tumors is better, but they still have only a 15% to 39% 5-year survival rate (3). Clearly, there is an urgent need for new therapies for this aggressive disease.

Both angiogenesis and signaling through the RAF/mitogen-activated protein (MAP)/extracellular signal-regulated kinase (ERK) kinase (MEK)/ERK (RAF/MEK/ERK) cascade play critical roles in the development of HCC. Antiangiogenesis therapies, which inhibit blood vessel formation, may hold promise in the treatment of HCC, because HCC tumors depend on a rich blood supply (4). In addition to being highly angiogenic, human HCC tumors have high expression and enhanced activity of MAP kinase (MAPK) compared with adjacent nonneoplastic liver (5). Furthermore, treatment of HCC cells with a MEK inhibitor reduced cell proliferation and induced apoptosis (6) and overexpression of activated MEK1 in HepG2 cells enhanced tumor growth *in vivo* (7). Therefore, inhibition of both angiogenesis and RAF/MEK/ERK signaling may represent an attractive approach for the treatment of HCC.

Sorafenib (Nexavar, BAY 43-9006) is a multikinase inhibitor that has shown efficacy against a wide variety of tumors in preclinical models (8). It has been shown to block tumor cell proliferation and angiogenesis by inhibiting serine/threonine kinases (c-RAF, and mutant and wild-type BRAF) as well as the receptor tyrosine kinases vascular endothelial growth factor receptor 2 (VEGFR2), VEGFR3, platelet-derived growth factor receptor (PDGFR), FLT3, Ret, and c-KIT (8, 9). It has also been reported that sorafenib induces apoptosis in human leukemia cells (10) and other human tumor cell lines (11) through the inhibition of the translation and down-regulation of myeloid cell leukemia-1 (Mcl-1), a Bcl-2 family member. A recent report by Rahmani et al. (10) showed that the inhibition of eIF4E phosphorylation by sorafenib in leukemia cells was independent of its activity on the MEK/ERK pathway and suggests a possible linkage between eIF4E and translational control of Mcl-1. The purpose of the studies reported here was to build an understanding of the mechanism of action of sorafenib in preclinical models of HCC. Direct effects of sorafenib on HCC tumor cells were evaluated *in vitro* in PLC/PRF/5 (p53-mutant, K-Ras-mutant, and B-Raf wild type) and HepG2 (p53 wild type, K-Ras-mutant, and B-Raf wild type) HCC cell lines. The antitumor efficacy and mechanism of action of sorafenib were also characterized *in vivo* using the PLC/PRF/5 HCC tumor xenograft model.

Requests for reprints: Li Liu, Department of Cancer Biology, Bayer HealthCare Pharmaceuticals, 400 Morgan Lane, West Haven, CT 06516. Phone: 203-812-6724; Fax: 203-203-6923; E-mail: li.liu.b@bayer.com.

doi:10.1158/0008-5472.CAN-06-1377

Materials and Methods

Compounds. Sorafenib [*N*-(3-trifluoromethyl-4-chlorophenyl)-*N*′-(4-(2-methylcarbamoyl pyridin-4-yl)oxyphenyl)urea] was synthesized at Bayer Corporation (West Haven, CT). U0126 was purchased from Calbiochem (San Diego, CA). Compounds were dissolved in 100% DMSO (Sigma, St. Louis, MO) and diluted with RPMI 1640 to the desired concentration with a final DMSO concentration of 0.1% for *in vitro* studies. DMSO was added to cultures at 0.1% (v/v) as a solvent control.

Cell lines. PLC/PRF/5 (p53 mutant) and HepG2 (p53 wild type) human HCC tumor cells were obtained from American Type Culture Collection (Rockville, MD) and cultured in RPMI 1640 containing 10% fetal bovine serum (FBS) in 5% CO_2 at 37°C. Unless otherwise indicated, cell culture reagents were obtained from Life Technologies, Inc. (Gaithersburg, MD).

CellTiter-Glo luminescent cell viability assay. Cells were plated at 3,000 per well in 96-well microtiter plates and incubated overnight at 37°C in a humidified incubator containing 5% CO_2. On the following day, compounds were added to wells and cultures were incubated for an additional 72 hours. Cell viability was determined using the CellTiter-Glo luminescent cell viability kit from Promega Corporation (Madison, WI) according to the manufacturer's instructions (12). The IC_{50} value, at which 50% of the cell growth inhibition compared with DMSO control, was calculated by nonlinear regression analysis using GraphPad Prism software (San Diego, CA).

Cell death detection ELISA^{Plus} assay. The Cell Death Detection ELISA^{Plus} kit (Roche, Mannheim, Germany) was used to measure DNA fragmentation as a marker for apoptosis according to the manufacturer's instructions (13). Cells were seeded in 96-well plates at 10,000 per well. After 24 hours, cells were dosed and grown for an additional 48 hours in RPMI 1640 with 10% FBS or 0.1% bovine serum albumin (BSA) in 5% CO_2 at 37°C. Cytoplasmic fractions of control and treated cells were transferred into streptavidin-coated 96-well plates and incubated with biotinylated mouse

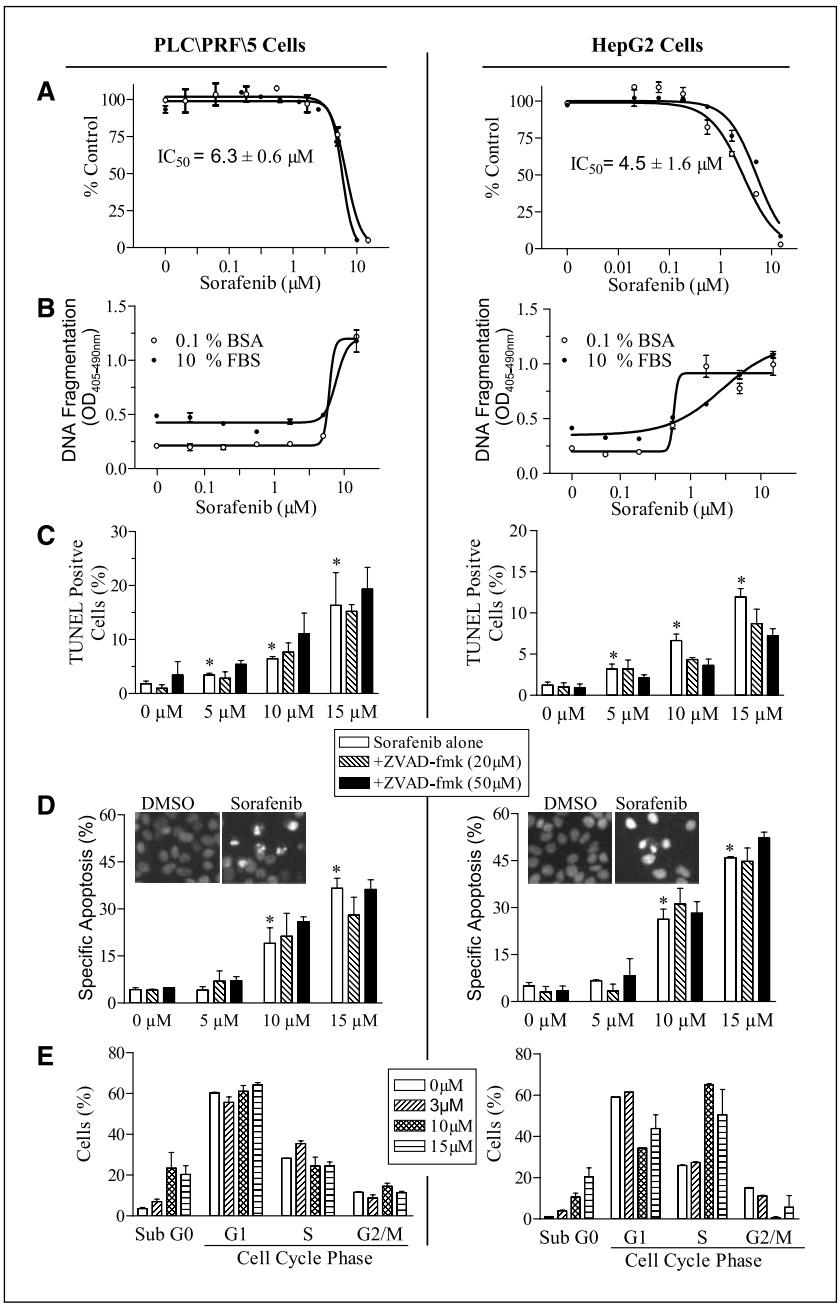

Figure 1. Sorafenib inhibits cell proliferation and induces apoptosis in HCC cells. *A,* inhibition of cell proliferation. Sorafenib was added to PLC/PRF/5 and HepG2 cells and cultured for 72 hours in RPMI 1640 containing 10% FBS. The experiment was done at least twice (○, experiment 1; ●, experiment 2). *B,* induction of DNA fragmentation detected by ELISA. Sorafenib was added to PLC/PRF/5 and HepG2 cells and cultured for 48 hours in complete culture medium in the presence of 10% FBS (●) or 0.1% BSA (○). *OD,* absorbance. *C,* TUNEL staining. Cells were treated with sorafenib in the presence of complete culture medium containing 10% FBS. ZVAD-fmk was added 2 hours before sorafenib treatment for 48 hours. Percentage of TUNEL-positive cells was quantified using Cellomic ArrayScan II image analysis system at ×40 magnification. *D,* Hoechst staining. Specific apoptotic cells, including both nuclear condensation and/or nuclear fragmentation phenotypes, were visualized and quantified using Cellomic ArrayScan II image analysis system. Assays were done in triplicate. *Columns,* mean (n = 3) of three independent determinations; *bars,* SE. *, $P < 0.05$, one-way ANOVA when compared with DMSO controls. *E,* cell cycle distribution. Cells were treated with sorafenib in the presence of complete culture medium containing 10% FBS for 24 hours and stained with propidium iodide. Cell cycle distribution was assessed using flow cytometry and quantified by Modfit software. The percentage of cells in G_1, S, or G_2-M phase was calculated after gating sub-G_0 population. Each value represents the percentage of cells in the noted cell cycle phases and is the average of two independent determinations. All results are representative of two separate experiments.

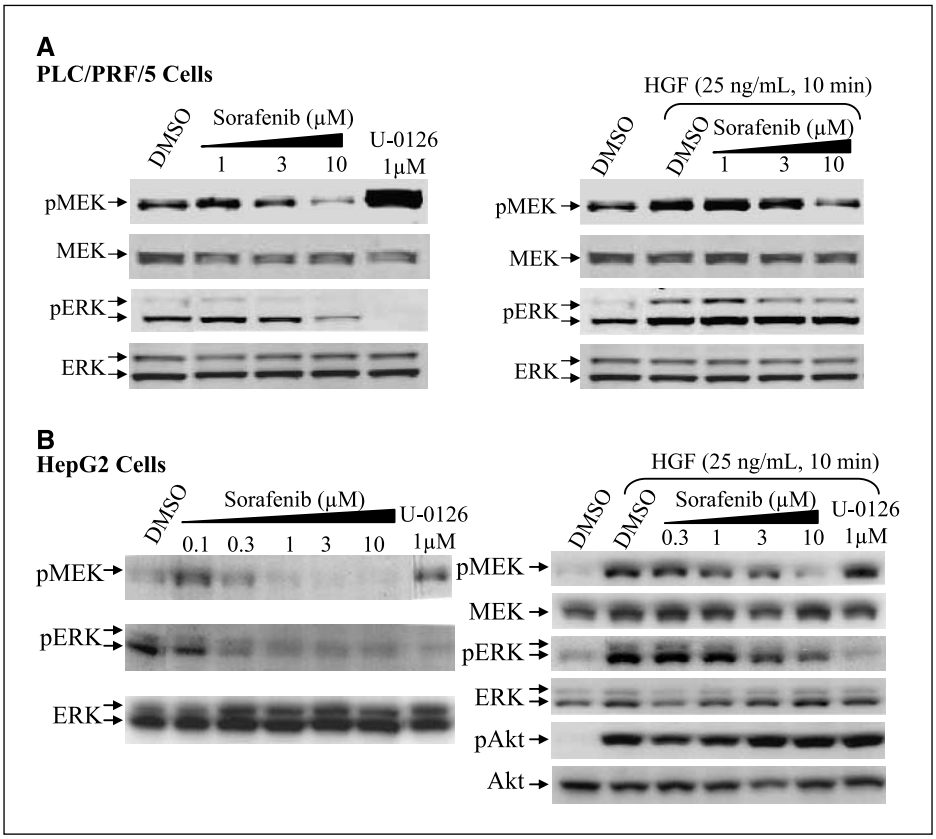

Figure 2. Sorafenib inhibits RAF/MEK/ERK signaling in PLC/PRF/5 (*A*) and HepG2 (*B*) cells. Cells were treated with compounds in RPMI 1640 with 0.1% BSA for 2 hours or followed by addition of hepatocyte growth factor (*HGF*; 25 ng/mL) for 10 minutes. Cells were lysed and 20 μg of soluble protein was separated by electrophoresis on a SDS-PAGE gel. Protein phosphorylation was detected by Western blot analysis.

antihistone antibody and peroxidase-conjugated mouse anti-DNA antibody at room temperature for 2 hours. Absorbance was determined at 405 to 490 nm using a Spectra Max Gemini microplate reader (Molecular Devices, Sunnyvale, CA).

Characterization of apoptosis morphology in cells. Cells were plated in 96-well plates at 3,000 cells per well. After compound treatment, cells were fixed using 10% buffered formalin/4% formaldehyde. Cellular DNA fragmentation morphology was detected by terminal deoxynucleotidyl transferase (TdT)–mediated nick end labeling (TUNEL) staining using ApopTag red *in situ* kit (Chemicon International, Inc., Temecula, CA) according to the manufacturer's directions. DNA nuclear morphology was examined with Hoechst 33258 dye (0.1 μg/mL) staining in fixed cells. Both TUNEL-positive cells and nuclear morphology phenotype were visualized and analyzed using Cellomic ArrayScan II image analysis system (Cellomics, Inc., Pittsburgh, PA).

Flow cytometry cell cycle analysis. Cells were plated in six-well plates at 3×10^5 per well. After compound treatment, cells were harvested by trypsinization and washed with PBS. Cells were fixed in ice-cold 80% ethanol, washed, and resuspended in 1 mL PBS; treated with 10 μL RNase A (21 mg/mL); and stained with 5 μL propidium iodide at 1 mg/mL for 30 minutes at room temperature. The stained cells were analyzed by flow cytometry (BD LSRII System, BD Biosciences, San Jose, CA) and DNA content was quantified using Modfit software (Verity Software House, Inc., Topsham, ME).

Immunoblot analysis. Cells were plated at 250,000 to 500,000 per well in six-well plates (Falcon multiwell, Becton Dickinson, Franklin Lakes, NJ). The following day, cells were treated with compounds in RPMI medium containing 10% FBS or 0.1% BSA for the times indicated in the experiment. After treatment, cells were washed with cold PBS and lysed in the culture dishes using cell lysis buffer [40 mmol/L Tris-HCl (pH 7.4), 10% glycerol, 50 mmol/L BGP, 5 mmol/L EGTA, 2 mmol/L EDTA, 0.35 mmol/L vanadate, 10 mmol/L NaF, and 0.3% Triton X-100] containing protease inhibitors (Complete Protease Inhibitor Tablets, Boehringer Mannheim, Indianapolis, IN). Twenty micrograms of protein, determined using Bio-Rad detergent-compatible protein assays, from control and treated cell lysates were loaded on 4% to 12% gradient NuPAGE gels (Novex, Inc., San Diego, CA), electrophoresed under reducing conditions, and transferred onto nitrocellulose membranes (0.45 μm; Bio-Rad Laboratories). Blots were probed with anti-phospho-ERK (Thr^{202}/Tyr^{204}, Cell Signaling Technology Inc., Beverly, MA), anti-phospho-MEK ($Ser^{217/221}$, Cell Signaling Technology), anti-phospho-eIF4E (Ser^{209}, Cell Signaling Technology), anti-phospho-AKT (Ser^{473}; Cell Signaling Technology), anti-cyclin D1 (Santa Cruz Biotechnology, Inc, Santa Cruz, CA), anti-Mcl-1 (Chemicon International), and horseradish peroxidase (HRP)–conjugated secondary antibodies (1:5,000), and then blots were developed with enhanced chemiluminescence reagent (Amersham, Piscataway, NJ) on Amersham Hyperfilm.

Tumor xenograft experiments. CB17 severe combined immunodeficient (SCID) female mice (Taconic Farms, Germantown, NY) were used for all *in vivo* studies. The mice were housed and maintained within the Comparative Medicine Department at Bayer Corporation, in accordance with Bayer Institutional Animal Care and Use Committee, State, and Federal guidelines for the humane treatment and care of laboratory animals. Mice received food and water *ad libitum*.

Tumors were generated by harvesting PLC/PRF/5 cells from mid-log phase cultures using trypsin-EDTA (Life Technologies). Cells were then pelleted and resuspended in a 50% mixture of Matrigel (BD Biosciences) in HBSS (Life Technologies) to a final cell count of 2.5×10^7/mL. A volume of 0.2 mL of the cell suspension was injected s.c. in the right flank of each mouse. Sorafenib tosylate was used for all *in vivo* experiments. Cremophor EL/95% ethanol (50:50; Sigma) was stored in the dark at room temperature. Sorafenib tosylate was formulated as previously described (8). Sorafenib tosylate was administered p.o., once daily for 16 or 21 days at dose levels of 10, 30, and 100 mg/kg body weight starting when all animals in the study had established tumors averaging from 140 to 160 mg with 10 mice per group.

Tumor dimensions and body weights were recorded twice weekly starting with the first day of treatment. Treatments producing >20% lethality and/or 20% net body weight loss were considered "toxic". Tumor

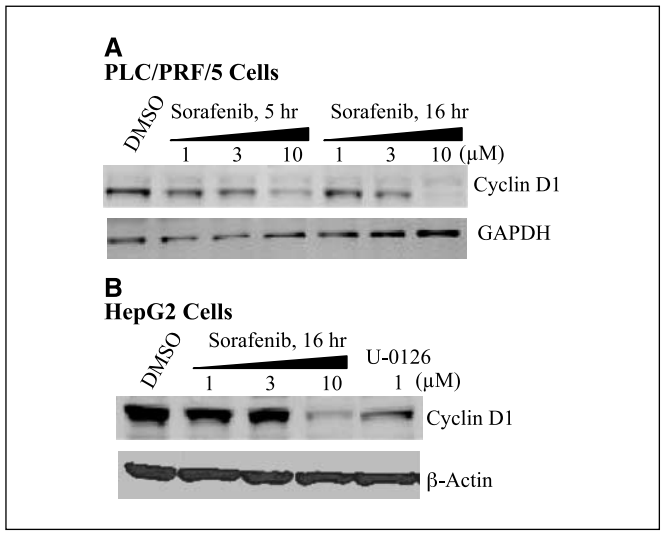

Figure 3. Sorafenib down-regulates cyclin D1 in HCC cells. PLC/PRF/5 (*A*) and HepG2 (*B*) cells were treated with compound for 5 or 16 hours in RPMI 1640 containing 10% FBS. After treatment, cells were lysed and 20 μg of soluble protein were separated by electrophoresis on a SDS-PAGE gel. Protein levels were detected by Western blot analysis. Glyceraldehyde-3-phosphate dehydrogenase (*GAPDH*) or β-actin was used as a loading control.

weights were calculated using the equation $(l \times w^2) / 2$, where l and w refer to the larger and smaller dimensions collected at each measurement. Antitumor efficacy was measured as the incidence of complete regressions (CR), partial regressions (PR), and tumor growth inhibition (TGI). CRs are defined as tumors that are reduced to below the limit of palpation. PRs are defined as tumors that are reduced by >50% but are <100% of their initial size. A minimum duration of 5 days is required for a CR or PR to be considered durable. TGI is defined as $[1 - (T/C) \times 100]$, where T and C are the mean tumor weight in the treated and untreated control groups, respectively, at the first measurement after the end of treatment. Tumor volume data were statistically analyzed with one-way ANOVA, and individual group comparisons were evaluated by Bonferroni's multiple comparison test. P values <0.05 were considered significant.

Mechanism of action studies and immunohistochemical staining and quantification. Female SCID mice with tumors measuring 200 to 300 mg in size received sorafenib tosylate p.o. once daily for 5 days at dose levels of 30 and 100 mg/kg. Tumors were harvested 3 hours after the last treatment. Tumors were either homogenized in tumor lysis buffer for Western blot analysis or fixed in paraformaldehyde for 24 hours, and paraffin sections were used for immunohistochemical staining. Immunohistochemical staining of paraffin sections of tumors was done with rat monoclonal anti-CD34 antibody (Abcam, Cambridge, MA) at a dilution of 1:50 (2 μg/mL) made in rabbit serum and rabbit monoclonal anti-phospho-ERK1/2 antibody (phospho-p44/42 MAPK, Thr^{202}/Tyr^{204}; Cell Signaling Technology) at a dilution of 1:60 made in antibody diluent (DakoCytomation, Fort Collins, CO). Staining was done using the Envision Plus HRP (3,3′-diaminobenzidine) system from DAKO (Carpinteria, CA) according to the manufacturer's protocol. The slides were counterstained with Mayer's hematoxylin for 1 minute and washed with water. TUNEL staining for mouse tumor tissue was based on the protocol of the TdT-Fragel DNA Fragmentation detection kit (Calbiochem).

The tissue sections were viewed at ×100 magnification and images were captured with a digital camera (Diagnostic Instruments, Inc., Sterling Heights, MI). Four fields per section were analyzed, excluding peripheral connective tissue and necrotic regions. Total tissue area analyzed in each section was 2.576 mm^2. Areas of CD34- or TUNEL-positive objects were quantified using ImagePro Plus version 3.0 (Media Cybernetics, Silver Spring, MD). Percentage of microvessel area (MVA) in each field was calculated as [(area of CD34-positive objects / measured tissue area) × 100]. Percentage of TUNEL-positive staining in each field was calculated as [(area of TUNEL-positive objects / measured tissue area) × 100]. Mean values of MVA- or TUNEL-positive area in each group were calculated from five tumor samples. Data were analyzed statistically with one-way ANOVA followed by Fisher's probable least-squares difference (StatView, version 4.5; Abacus Concepts, Inc., Berkeley, CA), where $P < 0.05$ was considered significant.

Results

Sorafenib inhibits proliferation and induces apoptosis in HCC cell lines. The effect of sorafenib on cell proliferation was measured by CellTiter-Glo (72 hours) assay and on apoptosis by using DNA fragmentation (48 hours) assays. Sorafenib inhibited cell proliferation dose-dependently with an IC_{50} of 6.3 μmol/L in PLC/PRF/5 and 4.5 μmol/L in HepG2 cells (Fig. 1*A*). Furthermore, sorafenib induced DNA fragmentation in both HCC cell lines in the presence of 10% FBS (PLC/PRF/5, EC_{50} = 7.7 μmol/L; HepG2, EC_{50} = 2.4 μmol/L) with no significant difference when done in the absence of serum (Fig. 1*B*).

Induction of apoptosis by sorafenib was further evaluated by TUNEL staining and by characterizing changes in nuclear morphology. Sorafenib increased TUNEL staining in a dose-dependent manner (Fig. 1*C*) in both HCC cell lines. Sorafenib (15 μmol/L) increased the percentage of TUNEL-positive cells from 1.8% and 1.2%, as seen in the controls, to 16.4% and 12.0% as seen in the treated PLC/PRF/5 and HepG2 cells, respectively. Pretreatment of

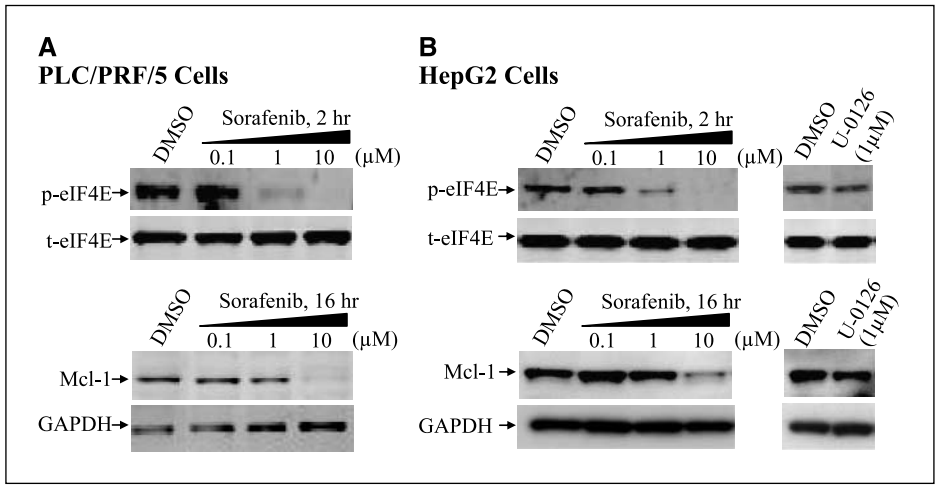

Figure 4. Sorafenib reduces phosphorylation of eIF4E and down-regulates Mcl-1 levels in HCC cells, independent of MEK/ERK. PLC/PRF/5 (*A*) and HepG2 (*B*) cells were treated with compound for 2 or 16 hours in RPMI 1640 with 10% FBS. After treatment, cells were lysed and 20 μg of soluble protein were separated by electrophoresis on a SDS-PAGE gel. Protein levels were detected by Western blot analysis. GAPDH or eIF4E was used as a loading control.

cells with a pan-caspase inhibitor, ZVAD-fmk, did not block sorafenib-induced apoptosis as measured by an increase in TUNEL staining in PLC/PRF/5 cells. However, it decreased sorafenib-induced TUNEL staining ~30% in HepG2 cells. Furthermore, both nuclear condensation and nuclear fragmentation (14), hallmarks of apoptosis, were detected using Hoechst staining of cells in both HCC cell lines after sorafenib treatment when measured at 48 hours of treatment. After treatment of PLC/PRF/5 cells with sorafenib, the majority of apoptotic cells displayed nuclear condensation and fragmentation (Fig. 1*D*). In contrast, the most prominent type of nuclear morphology present in sorafenib-treated HepG2 cells was nuclear condensation with little fragmentation observed (Fig. 1*D*). Pretreatment of cells with ZVAD-fmk had no significant effect on the nuclear morphologic changes induced by sorafenib in either HCC cell lines (Fig. 1*D*).

Cell cycle analysis by flow cytometry showed a decrease of G_1 and increase of S phase after sorafenib treatment for 24 hours in HepG2 cells, with less effects on cell cycle distribution observed in PLC/PRF/5 cells (Fig. 1*E*). Dose-dependent increases in the "sub-G_0" population, indicative of late-apoptotic or dead cells, were observed in both PLC/PRF/5 and HepG2 cells after treatment of sorafenib for 24 hours (Fig. 1*E*).

Sorafenib inhibits RAF/MEK/ERK signaling pathway in HCC cell lines. Raf kinases are best known as key regulators of the MEK/ERK cascade, and up-regulated signaling through the RAF/MEK/ERK pathway has an important role in HCC. Changes in the phosphorylation levels of key proteins in the RAF/MEK/ERK pathway were determined by Western blot analysis to evaluate the effect of sorafenib on this pathway in PLC/PRF/5 and HepG2 tumor cells. In both nonstimulated cells and hepatocyte growth factor–stimulated cells, sorafenib inhibited MEK and ERK phosphorylation at a concentration of between 3 and 10 μmol/L in PLC/PRF/5 cells (Fig. 2*A*) and between 1 and 3 μmol/L in HepG2 cells (Fig. 2B). The selective MEK inhibitor U0126, used as a control, inhibited ERK phosphorylation at 1 μmol/L while increasing the level of phospho-MEK, which is consistent with the induction of a feedback loop upon the inhibition of phospho-ERK and MAPK signaling in these cells. Total MEK, ERK, and AKT levels were unchanged, and no changes were observed in the phosphorylation levels of AKT.

The level of cyclin D1, which is involved in cell proliferation and is activated by both the RAF/MEK/ERK and phosphatidylinositol 3-kinase pathways in tumor cells (15, 16), was measured after 5 and 16 hours of sorafenib treatment to further characterize the effects of sorafenib on cell proliferation. At a concentration of 10 μmol/L, sorafenib reduced cyclin D1 protein level in both PLC/PRF/5 and HepG2 cells (Fig. 3). This seems to be a MEK/ERK–dependent effect as the selective MEK inhibitor U0126 also reduced cyclin D1 level in HepG2 cells.

The above data showed that sorafenib inhibited MEK and ERK phosphorylation and down-regulated cyclin D1 in both PLC/PRF/5 and HepG2 cells *in vitro*, consistent with the known inhibitory activity of sorafenib against Raf kinase isoforms.

Sorafenib reduces phosphorylation of eIF4E and down-regulates Mcl-1 levels in HCC cells, independent of MEK/ERK signaling. Mcl-1, an antiapoptotic member of the Bcl-2 family, has been shown to be an important factor for apoptosis resistance in HCC (17, 18). Sorafenib has been reported to induce apoptosis in human leukemia cells and other human tumor cell lines through the inhibition of translation and down-regulation of Mcl-1 (9, 10). Mcl-1 protein levels and the phosphorylation state of eIF4E were determined to understand if Mcl-1 could play a role in the mechanism of sorafenib-induced apoptosis in HCC cells. Sorafenib reduced the level of phospho-eIF4E after 2 hours of treatment at concentrations of 1 and 10 μmol/L (Fig. 4) in both HCC cell lines. Mcl-1 protein levels were also reduced after 16 hours at 10 μmol/L (Fig. 4) in both HCC cell lines. The MEK inhibitor U0126 had no effect on the level of eIF4E phosphorylation or Mcl-1 levels in HepG2 cells under the same conditions (Fig. 4). These data suggest that sorafenib reduces the phosphorylation of eIF4E and down-regulates Mcl-1 independent of its effects on MEK/ERK signaling.

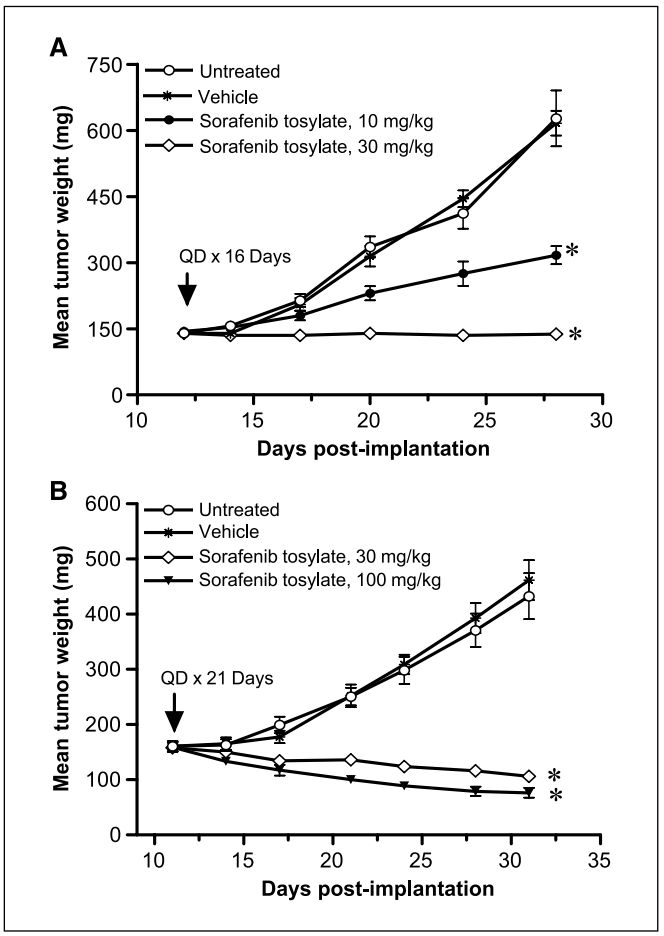

Figure 5. Sorafenib produces robust efficacy against PLC/PRF/5 HCC tumors in mice. PLC/PRF/5 tumors cells (5×10^6 per animal) were implanted s.c. in the flank of athymic mice as described in Materials and Methods in two independent experiments. Treatment was initiated on day 11 or 12 when all groups had tumors averaging 140 to 160 mg in size. Sorafenib tosylate was administered p.o. at 10, 30, or 100 mg/kg, qd × 16 days or qd × 21 days. There was no lethality in any group. Daily p.o. administration of sorafenib tosylate produced dose-dependent TGI and at 100 mg/kg; partial tumor regressions were observed in 5 of 10 animals. *Points,* mean tumor weight (n = 10); *bars,* SE. *, $P < 0.001$.

***In vivo* efficacy and mechanism of action of sorafenib against PLC/PRF/5 human HCC tumor xenografts.** Sorafenib tosylate produced dose-dependent growth inhibition of s.c. implanted PLC/PRF/5 tumor xenografts in SCID mice as shown in Fig. 5 and Table 1. Dose levels of 10 and 30 mg/kg produced significant and dose-dependent TGIs of 49% and 78%, respectively ($P < 0.001$; Fig. 5*A*). The effect at 30 mg/kg sorafenib tosylate was confirmed in an independent experiment ($P < 0.001$) and the dose response was further evaluated at a dose level of 100 mg/kg (Fig. 5*B*). Sorafenib tosylate produced durable partial tumor regressions in 50% of the mice at the 100 mg/kg dose level. It is

worth noting that establishment of s.c. PLC/PRF/5 tumors in SCID mice required implantation in a Matrigel matrix. Therefore, it is not possible to achieve complete tumor regressions in this model because the Matrigel would persist even if the tumor cells were completely eliminated. There was progressive moderate weight loss (6–17% of initial body weight) in the untreated and vehicle-treated control groups in these experiments. Weight loss was similar in the sorafenib-treated groups independent of the dose level, suggesting that weight loss was associated with tumor growth and not with drug treatment. These observations indicate that sorafenib was well tolerated and highly efficacious against this human HCC xenograft model.

The effects of sorafenib on angiogenesis and signaling through the RAF/MEK/ERK cascade, and on induction of apoptosis in PLC/PRF/5 mouse xenografts, were assessed in a separate experiment. PLC/PRF/5 xenograft tumors were generated as described previously. However, for this experiment, treatment was administered once daily for only 5 days, rather than for 16 or 21 days, and was not initiated until tumors were 200 to 300 mg in size. Larger tumors were required for this experiment so that when they were collected 3 hours after the last treatment, they could be bisected. Half of each tumor was formalin fixed for 24 hours and then analyzed by immunohistochemistry. The other half of each tumor was homogenized to generate lysates for Western blot analysis. CD34 is a specific endothelial cell marker and has been commonly used for microvessel quantification in HCC (19). Sorafenib tosylate at dose levels of 30 and 100 mg/kg significantly ($P < 0.001$) reduced tumor MVA in PLC/PRF/5 xenografts, as assessed by CD34 staining (Fig. 6*A*). Figure 6*A* also shows that sorafenib reduced ERK phosphorylation and induced tumor cell apoptosis, as measured by TUNEL staining, at both dose levels evaluated. The reduction in CD34 and increase in TUNEL-positive staining is quantified in the graphs shown in Fig. 6*C*. CD34 staining was reduced from 0.51% in the vehicle-treated tumors to 0.14% and 0.13% MVA in tumors treated with 30 or 100 mg/kg sorafenib, respectively. TUNEL staining in the same samples was increased from 0.07% positive area in the vehicle-treated tumors to 4.9% and 6.6% positive area in tumors treated with 30 or 100 mg/kg sorafenib, respectively. Tumor extracts from vehicle and sorafenib-treated groups were analyzed by Western blotting for phosphorylation levels of eIF4E. A dose-dependent reduction in p-eIF4E was observed in the tumor lysates from the animals treated with 30 and 100 mg/kg sorafenib (Fig. 6*B*). The observation that sorafenib reduced phospho-ERK and phospho-eIF4E levels and induced apoptosis in PLC/PRF/5 xenograft tumors is consistent with a direct effect of sorafenib on HCC tumor cell apoptosis in addition to its pronounced antivascular effect on tumor microvessel content.

Discussion

Sorafenib is a multikinase inhibitor with activity against the Ser/Thr kinase Raf, which is known to be important in tumor cell signaling and tumor cell proliferation, and several receptor tyrosine kinases involved in angiogenesis, including VEGFR2 and PDGFR. This multikinase inhibitor was recently approved for the treatment of advanced renal cell cancer based on the positive results of a large phase III randomized clinical trial and is currently under evaluation in phase III trials for malignant melanoma and HCC. In this report, we show in two human HCC cell lines that sorafenib blocks Raf kinase signaling, inhibits tumor cell proliferation, and induces apoptosis *in vitro*. In addition, sorafenib exhibits robust antitumor efficacy, including partial tumor regressions in PLC/PRF/5 HCC xenografts. The *in vivo* antitumor activity of sorafenib correlated with the inhibition of MAPK signaling, which is indicative of Raf kinase inhibition; induction of apoptosis as measured by TUNEL staining; and inhibition of tumor MVA (tumor angiogenesis) as measured by the reduction in CD34 staining. These results provide evidence that sorafenib may be an attractive approach for the treatment of HCC by simultaneously inhibiting both tumor angiogenesis (VEGF and PDGF signaling) and tumor cell survival (RAF kinase signaling-dependent and signaling-independent mechanisms).

Unlike other tumor types, most notably malignant melanoma, BRAF-activating mutations are relatively rare events in HCC (20, 21). However, Raf kinase is overexpressed in a high percentage of HCC patient tumors, and the RAF/MEK/ERK pathway can be activated by major etiologic factors such as HBV and HCV infection and mitogenic growth factors (21, 22). The data obtained in the present study indicate that sorafenib is able to inhibit Raf kinase and thus block MEK/ERK signaling in both PLC/PRF/5 and HepG2 cells. Like U0126, a selective MEK inhibitor, sorafenib reduced cyclin D1 level and inhibited cell proliferation in these two cell lines.

Table 1. Effect of sorafenib tosylate against s.c. PLC/PRF/5 human HCC xenografts

Sorafenib tosylate (mg/kg/dose)*	Experiment 1		Experiment 2	
	Percent TGI [(1 − *T/C*) × 100], qd × 21	Maximum percent net body weight loss	Percent TGI [(1 − *T/C*) × 100], qd × 16	Maximum percent net body weight loss
Control	−2	17	0	6
Vehicle	0	17	−7	8
10	49†	16	—	—
30	78†,‡	12	75†	12
100	—	—	82† (5/10 PR)	16

*Sorafenib tosylate was administered p.o. once daily for 16 or 21 days at dose levels of 10, 30, and 100 mg/kg when all animals in the study had established tumors averaging from 140 to 160 mg.
†$P < 0.001$, significantly different from the control group.
‡$P < 0.001$, significantly different from the 10 mg/kg dose level.

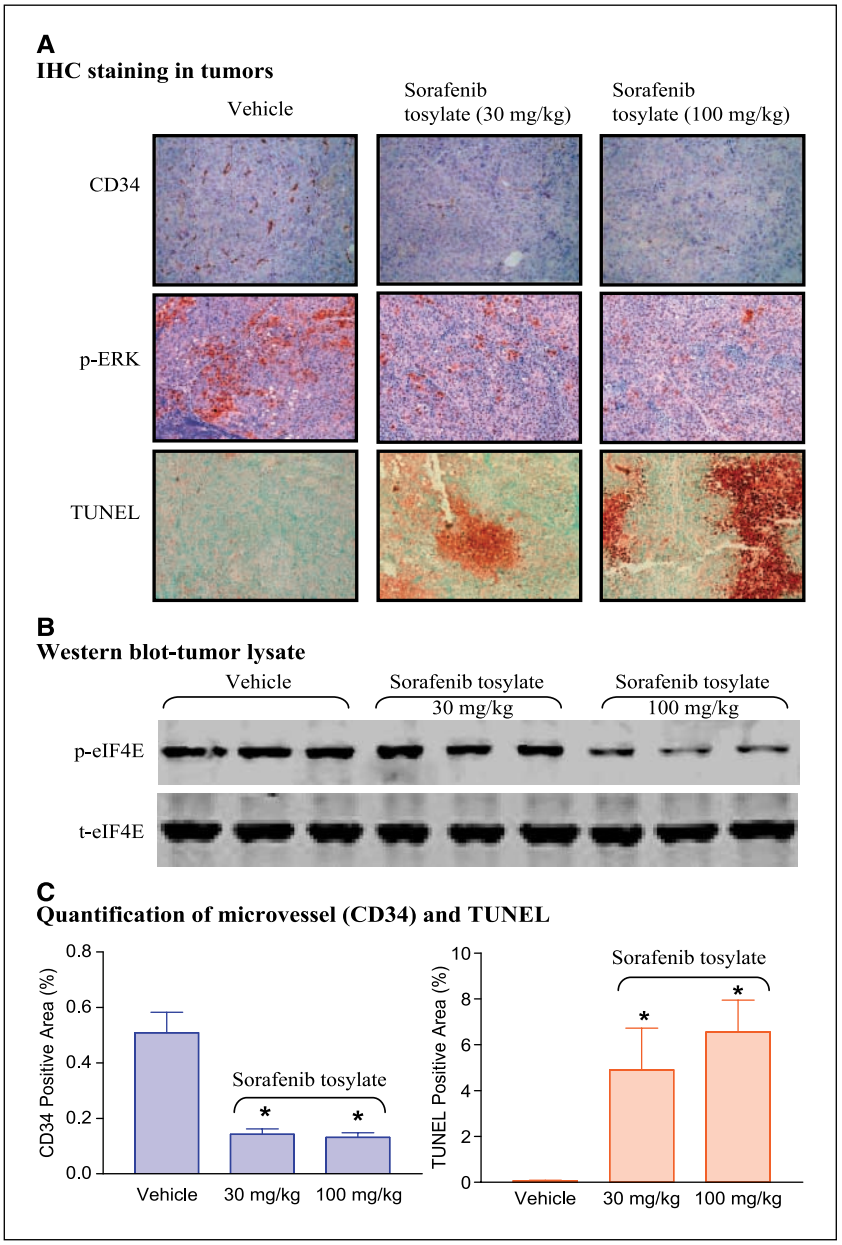

Figure 6. *In vivo* mechanism of action of sorafenib in PLC/PRF/5 HCC tumors. Sorafenib tosylate was administered once daily for 5 days at the indicated dose levels to female SCID mice with tumors measuring 200 to 300 mg in size. Tumors were collected 3 hours after the last treatment. Tumors were either homogenized for analysis by Western blot or formalin fixed for 24 hours and then analyzed by immunohistochemistry (*IHC*). *A,* sorafenib reduces the microvessel density, as measured by CD34 staining; the amount of phosphorylation of ERK, as measured by phosphospecific antibodies to phospho-ERK (*p-ERK*); and induces apoptosis, as measured by the increase in staining of TUNEL-positive area in PLC/PRF/5 tumors in mice. *B,* sorafenib reduces the phosphorylation level of eIF4E in PLC/PRF/5 HCC tumors in mice. *C,* quantification of microvessel (CD34 staining) and TUNEL-positive areas from immunohistochemical analysis of PLC/PRF/5 tumors. *Columns,* mean (five samples per group); *bars,* SE. *, $P < 0.05$, treated group versus vehicle group by one-way ANOVA Dunnet's multiple comparison test.

In addition to the inhibition of proliferation, sorafenib also induced apoptosis as measured by the increase in DNA fragmentation, TUNEL staining, nuclear fragmentation, and condensation in both PLC/PRF/5 and HepG2 cells. Sorafenib-induced apoptosis as assessed by TUNEL staining and nuclear morphology was not inhibited by a pan-caspase inhibitor, ZVAD-fmk, in PLC/PRF/5 cells (Fig. 1*C* and *D*) and only partially inhibited by ZVAD-fmk in HepG2 cells using TUNEL staining (Fig. 1*C*). We also observed that sorafenib-induced caspase-3 activation was detected in HepG2 cells but not in PLC/PRF/5 cells (data not shown). This suggests that sorafenib-induced apoptosis may not be dependent on caspases in PLC/PRF/5 cells. The induction of apoptosis by sorafenib through both caspase-dependent and caspase-independent pathways has been reported previously by Panka et al. (23) and although sorafenib induces apoptosis via different pathways in HepG2 and PLC/PRF/5 cells, both cell lines are equally sensitive to the compound *in vitro*.

Although the effects of sorafenib on caspase activation and cell cycle regulation differ between the HCC cell lines, sorafenib down-regulated the antiapoptotic protein Mcl-1 and reduced eIF4E phosphorylation in both lines. These effects were similar to those reported previously by Yu, Rahmani, and colleagues (10, 11) in other tumor cell lines. The down-regulation of Mcl-1 and eIF4E phosphorylation were not seen with the MEK inhibitor U0126 in HepG2 cells, suggesting that these effects are not mediated through the MEK/ERK pathway. Genetic evidence suggests that Raf-1 may regulate apoptosis in a manner independent of its kinase activity and ability to signal through the MEK/ERK pathway (24–26). Raf kinase is a member of a large protein complex that includes 14-3-3, RKIP, KSR, CNK, Spred, and SURB proteins (27, 28). It also regulates the activity of ASK1, BAG1, MST2, and nuclear factor-κB in a kinase-independent manner (26, 28–30). The mechanism underlying sorafenib-induced reduction of eIF4E phosphorylation and

Mcl-1 down-regulation remains to be elucidated but may involve regulation of translational control of Mcl-1 by an eIF4E-dependent mechanism (10).

Sorafenib has previously been reported to inhibit the growth of a wide variety of human tumor xenografts in mice (8). The antitumor effect of sorafenib can best be characterized as disease stabilization, and in many of these tumor models, it has been difficult to measure the relative contributions of the antiangiogenic activity of sorafenib versus its direct antitumor activity (8). In the current study, sorafenib significantly inhibited angiogenesis, phosphorylation levels of ERK and eIF4E, and induced cell death after only 5 days of treatment in PLC/PRF/5 tumors. This sorafenib-induced tumor apoptosis resulted in tumor shrinkage that develops slowly and progressively in this model and reached the level of objective regression after 10 days of dosing. These results suggest that both the antiangiogenic activity and the inhibition of the tumor cell signaling activity through Raf kinase–dependent and Raf kinase–independent pathways, including apoptosis induction, may contribute to the tumor regression observed in the PLC/PRF/5 tumor mice treated with sorafenib. Additional studies would be needed to assess the efficacy of sorafenib against HCC tumors grown orthotopically. Therefore, these data support the ongoing phase III clinical trials to assess the antitumor efficacy of sorafenib in HCC patients.

In summary, this study shows that sorafenib inhibits the RAF/MEK/ERK pathway both *in vitro* and *in vivo*, inhibits tumor angiogenesis, induces tumor cell apoptosis *in vivo*, and is efficacious against a model of human HCC in SCID mice. The inhibition of the RAF/MEK/ERK signaling pathway, the reduction of eIF4E phosphorylation, and the down-regulation of Mcl-1 protein levels may contribute to the proapoptotic effects of sorafenib in HCC tumors in addition to its pronounced antivascular effects. These observations may provide potentially useful biomarkers of sorafenib activity for the ongoing HCC clinical trials and/or rationale to combine with other chemotherapeutic agents.

Acknowledgments

Received 4/18/2006; revised 9/11/2006; accepted 10/17/2006.

The costs of publication of this article were defrayed in part by the payment of page charges. This article must therefore be hereby marked *advertisement* in accordance with 18 U.S.C. Section 1734 solely to indicate this fact.

We thank Drs. Lori-Ann Minasi and Ian Taylor for critical reading of the manuscript, Gwenda Ligon for RAF and RAS genotype analyses, David Wunderlich for fluorescence-activated cell sorting analysis, and Mark McHugh and Chien-Ping Shen for their assistance in apoptosis characterization.

References

1. Llovet JM, Burroughs A, Bruix J. Hepatocellular carcinoma. Lancet 2003;362:1907–17.
2. Bosch FX, Ribes J, Diaz M, Cleries R. Primary liver cancer: worldwide incidence and trends. Gastroenterology 2004;127:S5–16.
3. Takenaka K, Kawahara N, Yamamoto K, et al. Results of 280 liver resections for hepatocellular carcinoma. Arch Surg 1996;131:71–6.
4. Semela D, Dufour JF. Angiogenesis and hepatocellular carcinoma. J Hepatol 2004;41:864–80.
5. Schmidt CM, McKillop IH, Cahill PA, Sitzmann JV. Increased MAPK expression and activity in primary human hepatocellular carcinoma. Biochem Biophys Res Commun 1997;236:54–8.
6. Wiesenauer CA, Yip-Schneider MT, Wang Y, Schmidt CM. Multiple anticancer effects of blocking MEK-ERK signaling in hepatocellular carcinoma. J Am Coll Surg 2004;198:410–21.
7. Huynh H, Nguyen TT, Chow KH, Tan PH, Soo KC, Tran E. Over-expression of the mitogen-activated protein kinase (MAPK) kinase (MEK)-MAPK in hepatocellular carcinoma: its role in tumor progression and apoptosis. BMC Gastroenterol 2003;3:19.
8. Wilhelm SM, Carter C, Tang L, et al. BAY 43-9006 exhibits broad spectrum oral antitumor activity and targets the RAF/MEK/ERK pathway and receptor tyrosine kinases involved in tumor progression and angiogenesis. Cancer Res 2004;64:7099–109.
9. Carlomagno F, Anaganti S, Guida T, et al. BAY 43-9006 inhibition of oncogenic RET mutants. J Natl Cancer Inst 2006;98:326–34.
10. Rahmani M, Davis EM, Bauer C, Dent P, Grant S. Apoptosis induced by the kinase inhibitor BAY 43-9006 in human leukemia cells involves down-regulation of Mcl-1 through inhibition of translation. J Biol Chem 2005;280:35217–27.
11. Yu C, Bruzek LM, Meng XW, et al. The role of Mcl-1 downregulation in the proapoptotic activity of the multikinase inhibitor BAY 43-9006. Oncogene 2005;24:6861–9.
12. Wesiersk-Gadek J, Wojciechowski J. CellTiter-Glo Assay: application for assessing direct cytotoxicity and for determining cell proliferation and cell cycle regulation. Cell Notes 2003;6:251–306.
13. Wyllie AH, Kerr JF, Currie AR. Cell death: the significance of apoptosis. Int Rev Cytol 1980;68:251–306.
14. Cummings BS, Kinsey GR, Bolchoz LJ, Schnellmann RG. Identification of caspase-independent apoptosis in epithelial and cancer cells. J Pharmacol Exp Ther 2004;310:126–34.
15. Pruitt K, Der CJ. Ras and Rho regulation of the cell cycle and oncogenesis. Cancer Lett 2001;171:1–10.
16. Huynh H, Do PT, Nguyen TH, et al. Extracellular signal-regulated kinase induces cyclin D1 and Cdk-2 expression and phosphorylation of retinoblastoma in hepatocellular carcinoma. Int J Oncol 2004;25:1839–47.
17. Fleischer B, Schulze-Bergkamen H, Schuchmann M, et al. Mcl-1 is an anti-apoptotic factor for human hepatocellular carcinoma. Int J Oncol 2006;28:25–32.
18. Sieghart W, Losert D, Strommer S, et al. Mcl-1 overexpression in hepatocellular carcinoma: a potential target for antisense therapy. J Hepatol 2006;44:151–7.
19. Poon RT, Ng IO, Lau C, et al. Tumor microvessel density as a predictor of recurrence after resection of hepatocellular carcinoma: a prospective study. J Clin Oncol 2002;20:1775–85.
20. Karasarides M, Chiloeches A, Hayward R, et al. B-RAF is a therapeutic target in melanoma. Oncogene 2004;23:6292–8.
21. Tannapfel A, Sommerer F, Benicke M, et al. Mutations of the BRAF gene in cholangiocarcinoma but not in hepatocellular carcinoma. Gut 2003;52:706–12.
22. Hwang YH, Choi JY, Kim S, et al. Over-expression of c-raf-1 proto-oncogene in liver cirrhosis and hepatocellular carcinoma. Hepatol Res 2004;29:113–21.
23. Panka DJ, Wang W, Atkins MB, Mier JW. The Raf inhibitor BAY 43-9006 (Sorafenib) induces caspase-independent apoptosis in melanoma cells. Cancer Res 2006;66:1611–9.
24. Huser M, Luckett J, Chiloeches A, et al. MEK kinase activity is not necessary for Raf-1 function. EMBO J 2001;20:1940–51.
25. Mikula M, Schreiber M, Husak Z, et al. Embryonic lethality and fetal liver apoptosis in mice lacking the c-raf-1 gene. EMBO J 2001;20:1952–62.
26. Hindley A, Kolch W. Extracellular signal regulated kinase (ERK)/mitogen activated protein kinase (MAPK)-independent functions of Raf kinases. J Cell Sci 2002;115:1575–81.
27. Kolch W. Coordinating ERK/MAPK signalling through scaffolds and inhibitors. Nat Rev Mol Cell Biol 2005;6:827–37.
28. Malumbres M, Barbacid M. RAS oncogenes: the first 30 years. Nat Rev Cancer 2003;3:459–65.
29. O'Neill E, Rushworth L, Baccarini M, Kolch W. Role of the kinase MST2 in suppression of apoptosis by the proto-oncogene product Raf-1. Science 2004;306:2267–70.
30. Wellbrock C, Karasarides M, Marais R. The RAF proteins take centre stage. Nat Rev Mol Cell Biol 2004;5:875–85.

Sorafenib Blocks the RAF/MEK/ERK Pathway, Inhibits Tumor Angiogenesis, and Induces Tumor Cell Apoptosis in Hepatocellular Carcinoma Model PLC/PRF/5

Li Liu, Yichen Cao, Charles Chen, et al.

Cancer Res 2006;66:11851-11858.